MOLECULAR AND CELLULAR BIOLOGY, Jan. 2008, p. 131–139 Vol. 28, No. 1
0270-7306/08/$08.00+0 doi:10.1128/MCB.01119-07

The Alpha Catalytic Subunit of Protein Kinase CK2 Is Required for Mouse Embryonic Development[▽]

David Y. Lou, Isabel Dominguez, Paul Toselli, Esther Landesman-Bollag, Conor O'Brien, and David C. Seldin*

Departments of Medicine and Biochemistry, Boston University Medical Center, Boston, Massachusetts 02118

Received 23 June 2007/Returned for modification 13 July 2007/Accepted 6 October 2007

Protein kinase CK2 (formerly casein kinase II) is a highly conserved and ubiquitous serine/threonine kinase that is composed of two catalytic subunits (CK2α and/or CK2α′) and two CK2β regulatory subunits. CK2 has many substrates in cells, and key roles in yeast cell physiology have been uncovered by introducing subunit mutations. Gene-targeting experiments have demonstrated that in mice, the CK2β gene is required for early embryonic development, while the CK2α′ subunit appears to be essential only for normal spermatogenesis. We have used homologous recombination to disrupt the CK2α gene in the mouse germ line. Embryos lacking CK2α have a marked reduction in CK2 activity in spite of the presence of the CK2α′ subunit. CK2α$^{-/-}$ embryos die in mid-gestation, with abnormalities including open neural tubes and reductions in the branchial arches. Defects in the formation of the heart lead to hydrops fetalis and are likely the cause of embryonic lethality. Thus, CK2α appears to play an essential and uncompensated role in mammalian development.

CK2 is a ubiquitous and highly conserved serine/threonine kinase. With hundreds of putative substrates identified through in vitro studies (27), CK2 has been linked to fundamental cellular processes including the regulation of DNA transcription and damage responses (13, 14), protein translation and stability (5, 42), and circadian rhythms (22). Many studies have detected dysregulated expression of CK2 in human cancers (46). CK2 was found to be upregulated in lymphocytic pseudoleukemia in cattle infected by the parasite *Theileria parva* (32). We modeled this in transgenic mice that developed lymphoma with the overexpression of CK2α alone (40) or synergistically in collaboration with c-*myc*, Tal-1 overexpression (17), or p53 loss (19). We have found CK2α to be highly expressed in human and rodent mammary tumors, and transgenic expression of CK2α can also promote breast cancer in mice (20). These experiments validate the powerful role of CK2 in cellular growth control. However, to identify the essential functions of CK2, we and others have used gene targeting by homologous recombination.

CK2 genes were first deleted in yeast by homologous recombination. While mammals have two homologous catalytic subunits, CK2α and CK2α′, and a single regulatory subunit, CK2β, the fission yeast *Schizosaccharomyces pombe* has single catalytic and regulatory subunits. Orb5 is a mutant yeast strain in the catalytic CK2A1 subunit, and these yeasts have defects in polarized cell growth (41). Disruption of the regulatory CK2B1 subunit in *S. pombe* produces a cold-sensitive phenotype and abnormalities in cell shape (36). *Saccharomyces cerevisiae* has two catalytic and two regulatory subunits; temperature-sensitive alleles of CK2A1 show defects in cell polarity (35), and temperature-sensitive alleles of CK2A2 have defects in cell cycle progression with a dual-arrest phenotype at both the G_1 and G_2/M transitions (16). Deletion of CK2B1 leads to a salt-sensitive phenotype, indicating that the enzyme in yeast has a role in ion homeostasis (2). A genomic screen of the CK2 yeast mutants shows the dysregulation of hundreds of genes (1).

In mice, deletion of the single CK2β regulatory subunit by homologous recombination is early embryonic lethal in a cell-autonomous fashion (4). Precisely what fundamental cell process was blocked is unclear, because those investigators were unable to generate CK2β$^{-/-}$ embryonic fibroblasts or embryonic stem (ES) cells. In contrast, we found that the deletion of the minor CK2α′ catalytic subunit is well tolerated, as homozygous null CK2α′$^{-/-}$ mice are viable but the males are infertile (51). The developing spermatocytes are frequently defective and undergo apoptosis, leading to oligospermia; the surviving spermatozoa are abnormal and resemble those seen in the human infertility syndromes of "globozoospermia" (round-headed sperm). We have now targeted the more abundant CK2α subunit by homologous recombination. Mice lacking CK2α die in mid-gestation, with structural defects in heart and neural tube, highlighting the specific role of CK2α in the development of these organs.

MATERIALS AND METHODS

CK2α-targeting construct. Long-range PCR was used to amplify a total of 8.3 kb of genomic DNA from the 129SvEv BAC clone pBeLoBAC11-240o17 (Incyte Genomics) as 3.7- and 4.6-kb arms. Each arm was then sequentially cloned into pBluescriptII KS(+) and pPNT (23) targeting vectors. The 5′ arm (3.7 kb) spanned the translational start site to the second coding exon, ending upstream of the codon for lysine 68 (K68). The 3′ arm (4.6 kb) began 85 nucleotides downstream of the 5′ arm and spanned the next three exons, thereby deleting the K68 residue critical for ATP binding (Fig. 1A). The 5′ arm was amplified using the following PCR primers containing KpnI restriction sites: forward primer 5′-AAGGTACCAAGCAGGGCCAGAGTTTACA-3′ and reverse primer 5′-AAGGTACCCACTGTATT TGCCCCTACCTAA-3′. The 3′ arm was amplified using the following PCR primers with restriction sites (XhoI on the forward primer and SacI and NotI on the reverse primer): forward primer 5′-GGGATCTCGAGAGTTACTTGGAATGTAGAGT-3′ and reverse primer 5′-AATGAGCTCGCGGCCGCTTTAATTACA GTTCTATTGC-3′. Final concentrations of PCR components were as follows: 200 μM each deoxynucleoside triphosphate, 400 nM each primer, 1.8 mM Mg^{2+}, 1 U eLONGase enzyme mix (In-

* Corresponding author. Mailing address: Boston University Medical Center, 650 Albany Street, Boston, MA 02118. Phone: (617) 638-7027. Fax: (617) 638-7530. E-mail: dseldin@bu.edu.

▽ Published ahead of print on 22 October 2007.

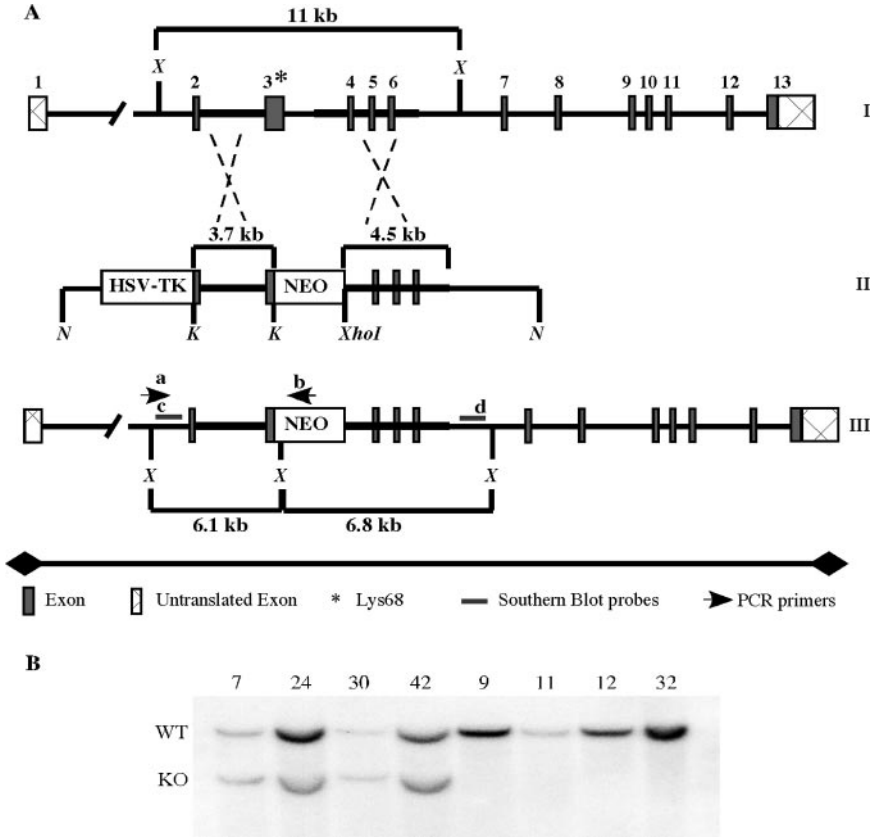

FIG. 1. CK2α targeting. (A) CK2α-targeting vector (II) and targeted allele (III). To generate a CK2α null allele, an 85-bp region of the gene (I) (numbers indicate exons) that included the critical K68 residue (*) in the catalytic ATP-binding pocket was targeted. A 3.7-kb 5′-flanking arm and 4.5-kb 3′-flanking arm were cloned into vector pPNT using KpnI (K), NotI (N), and XhoI. Screening was carried out by PCR using an external flanking and internal *neo* PCR primer pair (a and b, respectively). (B) To confirm homologous recombination, Southern blotting was carried out following XmnI (X) restriction digestion. A 5′-flanking probe (c) was used to identify the 11-kb wild-type (WT) and 6.1-kb homologously recombined DNA fragments, confirmed with a 3′ probe (d) (not shown). ES cell colonies 7, 24, 30, and 42 were hemizygous for the targeted CK2α allele, while colonies 9, 11, 12, and 32 were wild type. HSV, herpes simplex virus; KO, knockout.

vitrogen), and 500 ng DNA template. Thermocycling was performed for 35 cycles with denaturation at 94°C and annealing and extension at 68°C. Each flanking arm was individually cloned into pBluescriptII KS(+) (Stratagene) using KpnI for the 5′ arm and XhoI and SacI for the 3′ arm. The final CK2α-targeting construct was assembled by subcloning the 5′ and 3′ arms into pPNT using KpnI, XhoI, and NotI and confirmed by restriction mapping and PCR.

ES cell transfection, selection, and identification of homologous recombinants. TC1 ES cells, kindly provided by Philip Leder, were cultured in ES medium consisting of Dulbecco's modified eagle's medium (Cellgro) supplemented with 12.5% ES-grade fetal bovine serum (Sigma), 2% L-glutamine, 1% nonessential amino acids, 1% penicillin, and 1% streptomycin supplemented with 5×10^5 U Esgro-Lif (Chemicon) on mitomycin-treated mouse embryonic fibroblast feeder cells prepared from a neomycin-resistant mouse in a 7.5% CO_2 incubator at 37°C. ES cells (1×10^7 cells) were electroporated with 40 μg (1 μg/μl) of NotI-linearized targeting vector at 250 V and 250 μF, resuspended in 10 ml of ES medium, and evenly split into 10 10-cm tissue culture plates containing inactivated fibroblast feeder cells with ES medium without selection. Drug selection with 260 μg/ml G418 (Gibco) was started 24 h following transfection for 48 h, followed by the addition of 0.1 μM 1-(2-deoxy-2-fluoro-β-D-arabinofuranosyl)-5-iodouracil (FIAU) for an additional 96 h. Fresh drug-containing medium was changed daily. Undifferentiated drug-resistant ES colonies were picked when they reached the appropriate size and expanded for freezing and DNA analysis. ES cell DNA was prepared using the Qiagen DNeasy tissue kit according to the manufacturer's instructions. Homologous recombination was confirmed by PCR and Southern blotting. For the PCR, a 5′ primer upstream of the targeting arm, 5′-CK2aKO_F (5′-CCAACGTCT GCTTTTGAACA-3′), and a 3′ primer in the neomycin cassette, CK2aKO_R2 (5′-TCGCCT TCTTGACG AGTTCT-3′), were used. The PCR product was 4,357 bp in size and identified the CK2α knockout allele. The presence of the homologously recombined allele was confirmed by Southern blotting using [^{32}P]dCTP-labeled 5′ and 3′ DNA probes. Probes were radiolabeled using a hexanucleotide random priming mix (Invitrogen) and Klenow (NEB) fragment according to the manufacturers' protocols. For Southern blots, 20 μg of genomic DNA from tail DNA or ES cells was digested with XmnI, separated on 1% agarose gels, and transferred in 400 mM NaOH onto a Gene Screen Plus (Perkin-Elmer) by capillary flow. Hybridization with labeled probes was performed with QuikHyb hybridization solution (Stratagene) according to the manufacturer's protocol and exposed to Kodak film for 24 to 72 h.

Generation and genotyping of knockout mice. All animal experimentation was performed with the approval of the Boston University Medical Center IACUC. Mice were initially maintained in a two-way specific-pathogen-free barrier facility in microisolator cages; subsequent generations were transferred to a one-way facility. Targeted ES cell clones were microinjected into C57BL/6 blastocysts in the microinjection facility at Tufts-New England Medical Center. In all, 52 injected blastocysts were transplanted into three pseudopregnant recipient female mice, resulting in 18 chimeric mice. High-grade male agouti coat chimeras were identified and bred with wild-type C57BL/6 females to test for germ line transmission of the targeted CK2α allele. F_1 agouti offspring were screened by PCR and Southern blotting using tail DNA prepared by proteinase K digestion and high-salt extraction. Identification of CK2α$^{+/-}$ F_1 mice confirmed germ line transmission of the targeted CK2α allele; heterozygous F_1 mice were intercrossed to attempt to generate homozygous CK2α knockout mice in the F2 generation.

Embryo isolation and genotyping. For timed matings, heterozygous CK2α$^{+/-}$ mice were interbred, and the females were checked the next morning for vaginal plugs, which was estimated to be 0.5 days postconception and therefore equiv-

alent to embryonic day 0.5 (E0.5). Pregnant females were maintained in their breeding cages for the appropriate number of days and then sacrificed for embryo collection. Embryos were removed from the uterine horns and processed immediately: they were frozen for protein analysis, homogenized in TRIzol reagent (Gibco BRL) for RNA extraction, or fixed in fresh 4% glutaraldehyde for histology. Embryonic genomic DNA was extracted from yolk sacs using the DNeasy tissue kit (Qiagen) according to the manufacturer's instructions. Genotyping was performed using a three-primer PCR consisting of one forward primer, CK2aKO_del_F (5′-CCACCATGTCTGGCATTAAA-3′), and two reverse primers, CK2aKO_del_R (5′-TTCCCCTCTTTGACCACATC-3′) and CK2aKO_R2 (5′-TCGCCTTCTTGACGAGTTCT). Primers CK2aKO_del_F and CK2aKO_del_R amplified a 406-bp product only from the wild-type allele, and primers CK2aKO_del_F and CK2aKO_R2 amplified a 650-bp product only from the targeted allele. Thirty-five cycles of thermocycling were performed, with denaturation at 94°C, annealing at 57°C, and extension at 72°C.

Analysis of embryonic gene expression. Embryo RNA was pretreated with DNase I to digest contaminating genomic DNA. First-strand cDNA was synthesized using the iScript cDNA synthesis kit (Bio-Rad). For reverse transcription (RT)-PCR, the following primer sets were used: 5′-ATCAAGGAAGGCTTTAGCAAATGGG-3′ and 5′-GAACCTCGGATTCACATCGTGAGA-3′, amplifying a 159-bp product, for brachyury (50); 5′-CGGTGTCCAACACAGATCTG-3′ and 5′-TCTCTCGAGGTGGGTTGAC-3′, amplifying a 187-bp product, for ANF (50); 5′-TGAGGGAGAGCGCAGGCTCAAG-3′ and 5′-TGCTGTCCACGATGGACGTAAGG-3′, amplifying a 361-bp product, for myogenin (50); 5′-GCCAAGAAGCGGATAGAAGG-3′ and 5′-TGTGGTTCAGGGCTCAGTC-3′, amplifying a 499-bp product, for MLC-2V (28); and 5′-CAGACCTGAAGGAGACCT-3′ and 5′-GTCAGCGTAAACAGTTGC-3′, amplifying a 286-bp product, for MLC-2A (18). The following thermocycler conditions were used for brachyury, myogenin, and ANF: 4 min of initial denaturation at 95°C; 31, 33, or 35 cycles of amplification (25 s at 94°C, 30 s at 60°C, and 45 s at 72°C); a 6-min final extension at 72°C; and a hold at 4°C. The following thermocycler conditions were used for MLC-2A and MLC-2V: 4 min of initial denaturation at 95°C; 30, 32, or 34 cycles of amplification (30 s at 94°C, 30 s at 50°C, and 45 s at 72°C); a 10-min final extension at 72°C; and a hold at 4°C.

Histology and in situ hybridization. Histologic and in situ hybridization techniques were previously described (45, 51). Briefly, freshly dissected whole embryos were fixed for 2 h with 4.3% glutaraldehyde followed by overnight fixation with 1% osmium tetroxide, dehydrated, and embedded in plastic. Sections (1 to 2 μm) were cut and either deplasticized and stained with hematoxylin and eosin or stained with toluidine blue. For in situ hybridization, embryos were fixed in fresh 4% paraformaldehyde in phosphate-buffered saline overnight at 4°C. Following dehydration and paraffin embedding, 5-μm sections were cut, rehydrated, and hybridized with antisense riboprobes to *Csnk2a1*, *Csnk2a2*, and *Csnk2b* that had been radiolabeled with [^{35}S]UTP (51). Following hybridization, slides were exposed, developed, fixed, and photographed. Adjacent sections were stained with hematoxylin and eosin.

CK2 protein expression and activity. For immunoblotting and kinase assays, E10.5 embryos were washed in ice-cold phosphate-buffered saline and rapidly transferred to lysis buffer containing 40 mM Tris-HCl (pH 8.0), 1% Nonidet P-40, 125 mM NaCl, 1 mM NaF, 1 mM phenylmethylsulfonyl fluoride, 1 mM Na_3VO_4, and Sigma protease inhibitor cocktail, followed by centrifugation to remove debris. Yolk sacs were used for genotyping as described above. Protein was quantified by BCA assay (Pierce), and 15 μg was separated on 10% sodium dodecyl sulfate-polyacrylamide gels and transferred onto polyvinylidene difluoride membrane (Millipore). Monoclonal antibody for CK2α/CK2α′ was obtained from BD Biosciences, that for CK2β was obtained from Calbiochem, and that for actin was AC-15, from Sigma. Goat anti-mouse horseradish peroxidase-conjugated secondary antibody was obtained from Santa Cruz Biotechnology. Visualization was performed using ECL (Pierce). For CK2 kinase activity, 7.5 μg of protein was incubated with 0.1 mM CK2-specific peptide substrate RRREEETEEE (Sigma-Genosys Inc.) in CK2 kinase buffer (100 mM Tris [pH 8.0], 20 mM $MgCl_2$, 100 mM KCl, 100 μM Na_3VO_4, 5 μCi [γ-^{32}P]GTP) at 30°C for 20 min. Control reactions were carried out without peptide. The reaction was stopped by adding 10 mM ATP in 0.4 N HCl. Samples were spotted onto P81 Whatmann filters and washed in 150 mM H_3PO_4 to remove unincorporated [γ-^{32}P]GTP, and phosphorylated peptides were measured by scintillation counting. Samples were assayed in duplicate, and background kinase activity in the absence of the peptide substrate was subtracted. *P* values were assessed by analysis of variance; Bonferroni correction was applied for multiple comparisons.

TABLE 1. Yield of live births from $CK2\alpha^{+/-} \times CK2\alpha^{+/-}$ matings[a]

Genotype	Expected frequency if viable	Expected frequency if lethal	No. of animals	Observed frequency
$CK2\alpha^{+/+}$	0.25	0.33	80	0.33
$CK2\alpha^{+/-}$	0.5	0.67	163	0.67
$CK2\alpha^{-/-}$	0.25	0	0	0

RESULTS

CK2α gene targeting. We generated mice in which the CK2α gene was disrupted by replacing the exon encoding the critical ATP-binding residue, lysine 68 (30), with a neomycin resistance cassette. The targeting construct, pPNT-CK2αKO (Fig. 1A), was linearized by NotI digestion and electroporated into TC1 ES cells. Transfected ES cells were subjected to positive and negative selection in G418 and FIAU, and colonies that survived double selection were screened by PCR for homologous recombination. Four out of the first 40 ES colonies screened were identified as being potential homologous recombinants (results not shown). This result was confirmed by Southern blotting (Fig. 1B). Clone 7 was chosen for injection into C57BL/6 embryos; high-grade chimeras were obtained and mated to wild-type C57BL/6 females. The presence of agouti F_1 offspring demonstrated that targeted ES cells contributed to the germ line, and the positive identification of $CK2\alpha^{+/-}$ F_1 mice by both PCR and Southern blotting confirmed germ line transmission of the knockout allele (not shown).

$CK2\alpha^{-/-}$ embryos are nonviable. All of the $CK2\alpha^{+/-}$ F_1 mice were viable, indistinguishable from their $CK2\alpha^{+/+}$ littermates, and fertile. $CK2\alpha^{+/-}$ mice were intercrossed to generate F_2 progeny. These progeny were screened by PCR and Southern blotting for the presence of the homologously recombined allele. Out of 243 F_2 mice genotyped from more than 30 litters, no $CK2\alpha^{-/-}$ mice were recovered at weaning (Table 1). The ratio of $CK2\alpha^{+/+}$ to $CK2\alpha^{+/-}$ pups at weaning was 1:2, consistent with the expected frequency for an embryonic lethal phenotype of $CK2\alpha^{-/-}$ mice, with no selection against $CK2\alpha^{+/-}$ births.

$CK2\alpha^{-/-}$ embryos lack CK2α transcript and protein and have diminished CK2 kinase activity. To determine whether the CK2α-null allele generated mRNA transcript and protein products, embryos ($CK2\alpha^{+/+}$, $CK2\alpha^{+/-}$, and $CK2\alpha^{-/-}$ littermates) were collected at E10.5. Genotyping of each embryo was performed by PCR of genomic DNA extracted from the corresponding yolk sacs. $CK2\alpha^{-/-}$ embryos were pooled, and mRNA was prepared for amplification by RT-PCR. No CK2α mRNA transcripts were detected in the $CK2\alpha^{-/-}$ embryos (Fig. 2A). Protein analysis performed on individual embryos indicated that the $CK2\alpha^{-/-}$ embryos lacked any detectable CK2α protein (42 kDa) but had amounts of CK2α′ protein (38 kDa) that were similar to those of their littermates, indicating that there was no compensatory upregulation of CK2α′ (Fig. 2B). However, CK2β levels were reduced in the knockouts (data not shown). The $CK2\alpha^{+/-}$ embryos consistently expressed approximately half the amount of CK2α protein compared to their $CK2\alpha^{+/+}$ littermates (Fig. 2B). CK2 kinase activity was measured using a specific CK2 peptide substrate

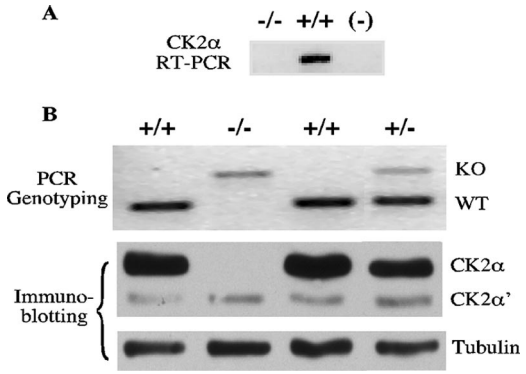

FIG. 2. CK2α$^{-/-}$ embryos lack CK2α mRNA and protein. (A) To detect CK2α mRNA transcripts, E10.5 embryos were genotyped individually by PCR using DNA prepared from the yolk sacs. Three CK2α$^{-/-}$ (−/−) and three CK2α$^{+/+}$ (+/+) embryos were pooled, and RT-PCR was performed; − indicates CK2α$^{+/+}$ RNA without RT. (B) To assay for CK2α protein, E10.5 embryos were genotyped, and protein extracts were prepared. Fifteen micrograms of protein from individual embryos was resolved by 10% sodium dodecyl sulfate-polyacrylamide gel electrophoresis and immunoblotted using an anti-CK2α/CK2α′ antibody. Wild-type CK2α$^{+/+}$ (+/+) embryos contained a major immunoreactive band at ~42 kDa, consistent with CK2α, and a weaker band at ~38 kDa, consistent with CKα′. In the knockout (KO) CK2α$^{-/-}$ (−/−) embryos, the intensity of the CK2α′ band was unchanged, and the CK2α band was absent. Heterozygote CK2α$^{+/-}$ (+/−) embryos reproducibly had a CK2α band of half the intensity of the wild type (WT). Tubulin was used as a loading control.

and [γ-^{32}P]GTP as a phosphate donor. Activity in the CK2α$^{+/-}$ embryos was 68% of that of the CK2α$^{+/+}$ embryos (P = 0.0002), and in the CK2α$^{-/-}$ embryos, it was 23% (P = 0.0001).

Developmental defects in CK2α$^{-/-}$ embryos. Timed matings were performed to determine when the CK2α$^{-/-}$ embryos die. A total of 155 embryos including 27 CK2α$^{-/-}$ embryos were examined. Throughout development, the CK2α$^{+/-}$ embryos were indistinguishable from CK2α$^{+/+}$ embryos. Beginning at E8.5, developmental abnormalities were observed in CK2α$^{-/-}$ embryos (Fig. 3A and B). While the CK2α$^{-/-}$ embryos had normal anteroposterior length at E8.5, their primitive hearts were enlarged in comparison to those of CK2α$^{+/+}$ embryos, and their neural folds were convex, while the neural folds of the CK2α$^{+/+}$ embryos had elevated and begun to fuse (Fig. 4A).

By E9.5, the abnormalities in the CK2α$^{-/-}$ embryos became more apparent (Fig. 3C and D). At this stage, blood is normally seen circulating in the yolk sac and the embryo, indicating that hematopoiesis has begun and that the primitive heart tube is circulating blood, and we observed this in the CK2α$^{+/+}$ and CK2α$^{+/-}$ embryos. However, even though the CK2α$^{-/-}$ hearts were contracting, they were enlarged in relation to the size of the embryo and appeared distended. Defects in the neural tube and head region of CK2α$^{-/-}$ embryos were variable in severity; typically, the rostral end was closed, but closure of the cranial portion failed to occur (Fig. 4B), while in a few embryos, the entire neural tube was open (craniorachischisis) (Fig. 4C). The head shape was abnormal, and the forebrain, midbrain, and hindbrain regions of CK2α$^{-/-}$ embryos were consistently smaller than those of their wild-type counterparts; there

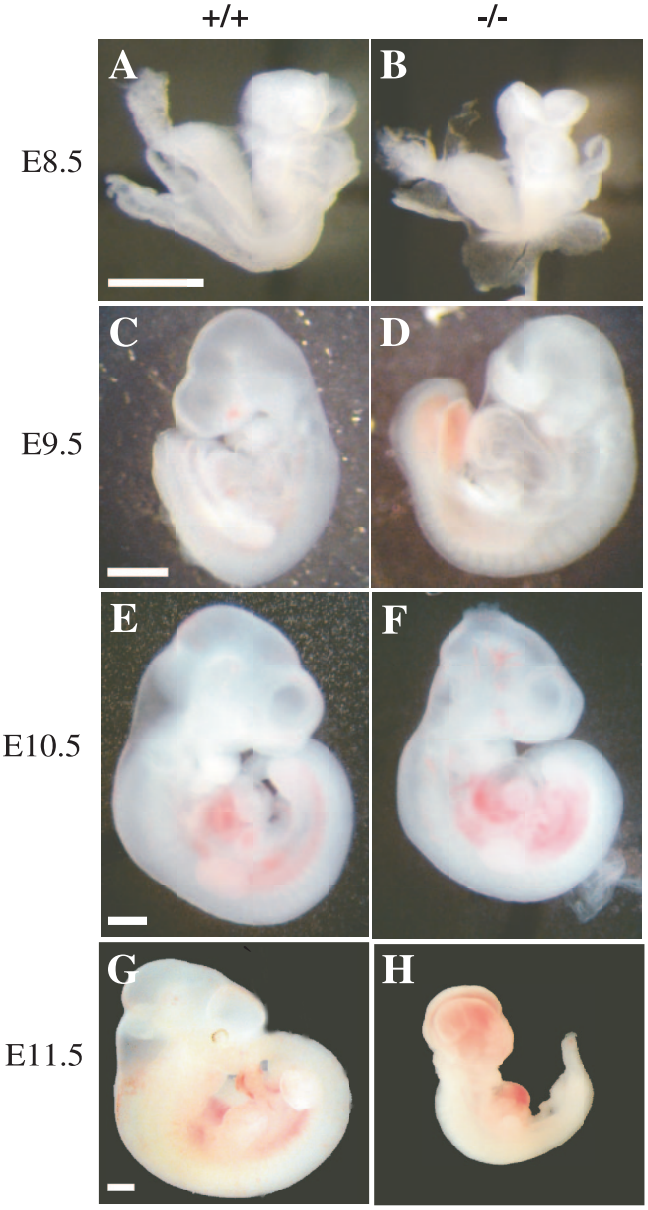

FIG. 3. Comparison of wild-type CK2α$^{+/+}$ (A, C, E, and G) and knockout CK2α$^{-/-}$ (B, D, F, and H) embryos from E8.5 to E11.5; white scale bars (500 μm) indicate the relative sizes of embryos between developmental stages. At E8.5 (A and B), the neural folds in the CK2α$^{-/-}$ embryos failed to elevate like those of CK2α$^{+/+}$ littermates. By E9.5 (C and D), CK2α$^{-/-}$ hearts were larger than those of their littermates; CK2α$^{-/-}$ neural tubes failed to fuse at the cranial level. At E10.5 (E and F), CK2α$^{-/-}$ embryos were usually smaller, hearts were dilated, and head shape was abnormal. At E11.5 (G and H), CK2α$^{-/-}$ embryos were runted, hearts were no longer were beating, and blood could be seen hemorrhaging into the cranium and thorax.

was no expansion of the telencephalic vesicles. The eye fields were identifiable but indistinct and underdeveloped in the CK2α$^{-/-}$ embryos, and the second branchial arch was usually underdeveloped (Fig. 4D to F and Table 2). Limb bud differentiation was delayed in CK2α$^{-/-}$ embryos compared with wild-type embryos. The tailbud of the CK2α$^{-/-}$ embryos was short and terminated in a broad, blunt end instead of a tapered

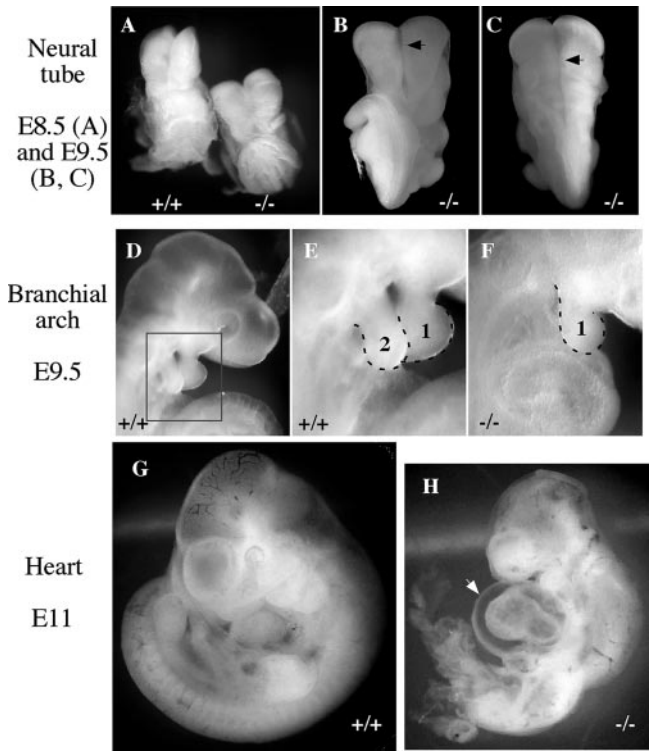

FIG. 4. Details of developmental defects in CK2α$^{-/-}$ embryos. (A to C) At E8.5, CK2α$^{-/-}$ neural folds failed to elevate (A). At E9.5, the neural folds failed to fuse along the anterior-posterior axis (arrows indicate the unfused neural tube on the ventral side [B] or dorsal side [C]). (D to F) By E9.5, wild-type embryos have developed the second branchial arch (D) (inset is enlarged in panel E), but it was smaller in most of the CK2α$^{-/-}$ embryos (F) (Table 2). (G and H) At E11, the pericardial sacs of the CK2α$^{-/-}$ embryos were edematous (arrow) due to heart failure, i.e., hydrops fetalis.

end as in the wild-type. Because of the cranial and tailbud defects, the CK2α$^{-/-}$ embryos were reduced in their anteroposterior lengths.

By E10.5, the CK2α$^{-/-}$ embryos were significantly smaller than littermate controls (Fig. 3E and F) when matched for somite number. Their hearts were contracting, and blood was circulating, but hearts were enlarged (E11) (Fig. 4G and H). Pericardial effusions, a sign of high-output cardiac failure, were sometimes seen in CK2α$^{-/-}$ embryos. The heads of CK2α$^{-/-}$ embryos remained smaller and malformed; the neural tubes remained open in this region, and the eye fields were underdeveloped, but the otic placodes were present. At matched developmental stages, the numbers of branchial arches were reduced in the knockout embryos (Table 2).

The CK2α$^{-/-}$ embryos did not progress beyond E10.5, and at E11.5, CK2α$^{-/-}$ embryos were not much bigger than normal E10.5 embryos (Fig. 3G and H). The branchial arches did not fuse, and the mouth was not formed. The optic vesicles, lens placodes, and retinal pigmentation were visible in wild-type embryos but were less pronounced in some CK2α$^{-/-}$ embryos and virtually absent in others. Limb bud development was retarded in the CK2α$^{-/-}$ embryos and never progressed beyond the limb bud paddle. At this stage, the hearts were large and dilated and no longer beating. Some of the embryos hemorrhaged into the thorax, abdomen, and cranium. Beyond E11.5, only a few necrotic CK2α$^{-/-}$ embryos could be identified.

Histological abnormalities in CK2α$^{-/-}$ embryos. Histologic sections were examined to determine the morphological basis of the neural tube and cardiac abnormalities seen in the developing embryos. Representative cranial and thoracic sections of E10.5 embryos demonstrated that the CK2α$^{-/-}$ embryos had an open neural tube in the forebrain region, although it was closed but collapsed in the region of the hindbrain (Fig. 5A and B). The rudiments of the telencephalic vesicles in the forebrain did not expand outward, and the optic stalk and evagination of the optic vesicle were collapsed. The otic vesicles were rounder in the CK2α$^{-/-}$ embryos, lacking the dorsal extension seen in normal embryos, and the epithelium was thickened. The notochord, trigeminal ganglion, and facioacoustic neural crest complex were present. Using both transmission electron microscopy and high-magnification light microscopy, mitoses were seen in both CK2α$^{+/+}$ and CK2α$^{-/-}$ embryos, indicating that the cells were viable and proliferating at this stage (not shown).

Transverse sections at the level of the thorax were also obtained in the same embryos. At this stage, the wild-type embryo was forming a four-chambered heart with trabeculation in the ventricles (Fig. 5C). In contrast, in CK2α$^{-/-}$ embryos, an open heart tube persisted, with an enlarged endomyocardial cavity with a thin and disorganized endothelial lining and reduced trabeculation and with a thin atrial wall. The surface ectoderm and presumptive parietal pericardial layer also appeared abnormal (Fig. 5D).

Markers of differentiation in CK2α$^{-/-}$ embryos. To begin to correlate molecular markers with the observed phenotypes in CK2α$^{-/-}$ embryos, we examined the expression of mRNA-encoding genes involved in mesoderm formation (brachyury and myogenin) and cardiac specification (MLC-2A, MLC-2V, and ANF) by semiquantitative RT-PCR (Fig. 6A). The number of amplification cycles was varied to ensure that the PCR was linear. Consistent with the phenotype of the mutant embryos, brachyury and myogenin were present in the CK2α$^{-/-}$ embryos, suggesting that gastrulation and the establishment of the mesoderm had taken place. Similarly, markers of heart development were present, suggesting that cardiomyocyte differentiation had begun in the CK2α$^{-/-}$ embryos. Hypoxanthine phosphoribosyltransferase was used as an internal control and demonstrated equal amounts of starting cDNA template between CK2α$^{-/-}$ and CK2α$^{+/+}$samples (Fig. 6A).

Expression pattern of CK2 mRNA transcripts in embryonic heart. We examined the pattern of mRNA expression of the CK2 subunits in normal heart development using in situ hybridization (Fig. 6B). In situ hybridization for CK2 subunit

TABLE 2. Branchial arches in embryos at E10.5

Genotype	Total no. of embryos counted	% of embryos with number of branchial arches of:			
		4	3	2	1
CK2α$^{+/+}$	18	78	22	0	0
CK2α$^{+/-}$	16	69	19	13	0
CK2α$^{-/-}$	14	25	36	50	7

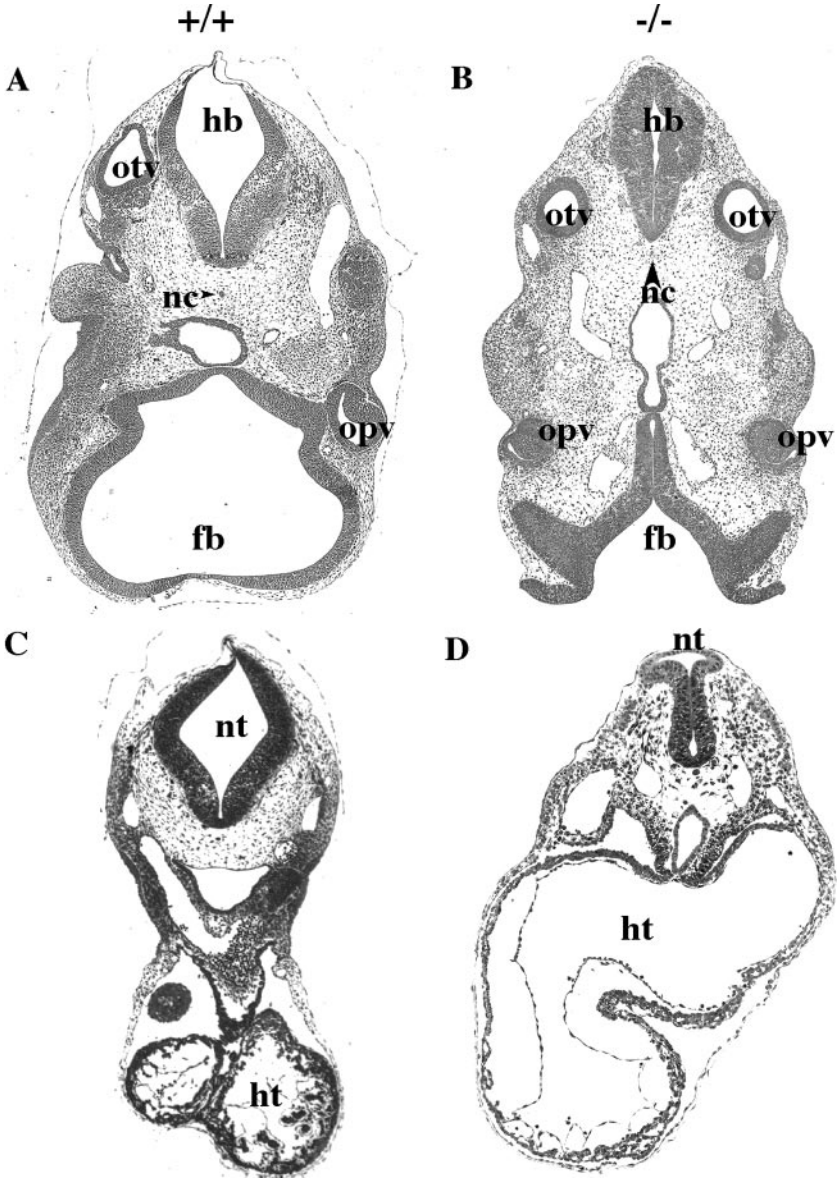

FIG. 5. Histological abnormalities in CK2α$^{-/-}$ embryos. Representative E10.5 CK2α$^{+/+}$ and CK2α$^{-/-}$ embryos were fixed and sectioned through the cranial (A and B) and thoracic (C and D) regions. In the CK2α$^{+/+}$ head (A), the neural tube has fused, forming a sealed tube that is expanding in preparation for brain development. In the CK2α$^{-/-}$ embryo, because the neural tube (nt) is open anteriorly in the forebrain (fb) region, the posterior tube has collapsed, interfering with the normal development of the hindbrain (hb). The optic vesicles (opv) and the notochord (nc) appear to be similar, but the otic vesicles (otv) in the CK2α$^{-/-}$ embryo are round and thickened compared to those in the CK2α$^{+/+}$ embryo, which has a characteristic dorsal extension. (C and D) Whereas the CK2α$^{+/+}$ heart (ht) is forming chambers and developing trabeculation, the heart of the CK2α$^{-/-}$ embryo is still an open tube.

transcripts demonstrated strong relative expression of CK2α mRNA in the ventricles at E13.5, while CK2α′ and CK2β appeared to have more uniform expression throughout the heart and the rest of the embryo.

DISCUSSION

We have demonstrated that CK2α$^{-/-}$ mice die in mid-embryogenesis, while CK2α$^{+/-}$ mice appear to be completely normal. The CK2α$^{-/-}$ embryos exhibited extensive cardiac and neural tube defects, and the embryonic lethality is likely attributable to abnormalities in the structure and function of the heart. Embryonic hearts were defective in CK2α$^{-/-}$ embryos isolated from E8.5 to E10.5, although they were able to beat. Sections of the CK2α$^{-/-}$ hearts revealed defective formation of the chambers and poor trabeculation. The CK2α$^{-/-}$ embryos died at ~E11, an age consistent with lethality due to defects in cardiac looping and chamber formation (6). Our RT-PCR results showed that transcript levels of the axial mesodermal marker brachyury and the striated muscle transcription factor myogenin were present but somewhat diminished in CK2α$^{-/-}$ embryos compared to wild-type embryos. In con-

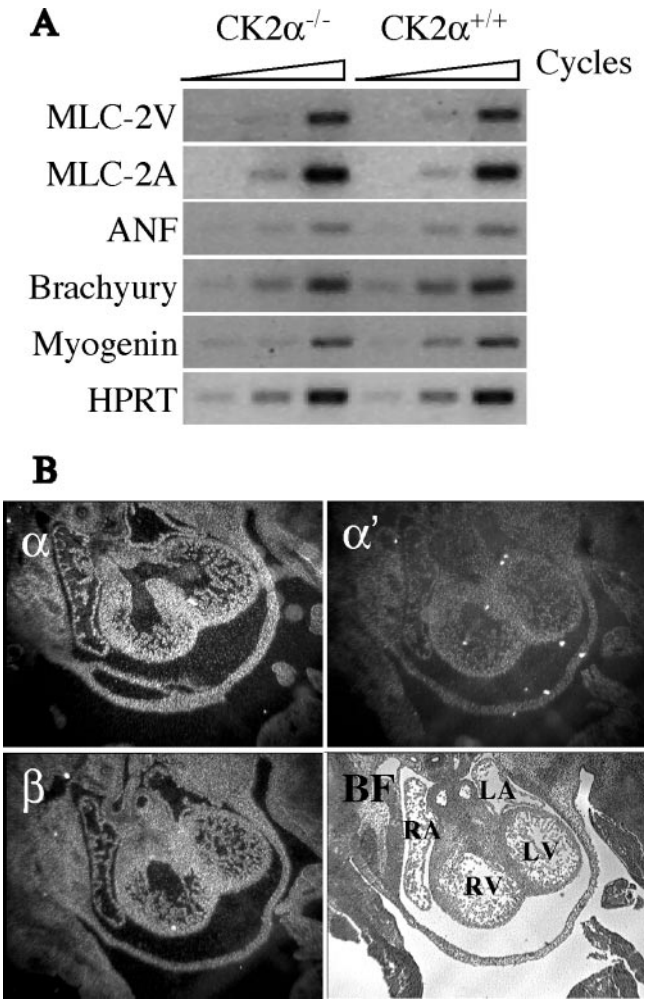

FIG. 6. mRNA expression in the embryos. (A) Semiquantitative RT-PCR was used to demonstrate the presence of mRNA encoding markers of mesoderm and cardiac formation in CK2α$^{-/-}$ and CK2α$^{+/+}$ embryos at E9.5. The triangles indicate increasing numbers of amplification cycles. Transcript levels of the cardiac markers MLC-2V, MLC-2A, and ANF and brachyury and myogenin, markers of mesoderm formation, were measured; hypoxanthine phosphoribosyltransferase (HPRT) was used as an mRNA control. (B) In situ hybridization for CK2 subunit transcripts demonstrates strong relative expression of CK2α mRNA in the ventricles at E13.5, while CK2α′ and CK2β appear to have a more uniform expression throughout the embryo. Sense probes showed no signal and are omitted, and a bright-field (BF) image is shown for orientation, with the right atrium (RA), left atrium (LA), right ventricle (RV), and left ventricle (LV) labeled.

trast, transcripts for cardiac markers such as MLC-2A, MLC-2V, and ANF were unchanged. Thus, the defect in the CK2α$^{-/-}$ embryos is not due to a global defect in mRNA transcription.

The heart is the first organ to develop, and it is essential for embryonic development. The process of cardiogenesis is complex but begins with the specification of the cardiac mesoderm. The primitive heart tube develops from this specialized tissue and progresses through a tightly regulated series of morphological changes including looping of the heart tube, emergence of the endocardial cushion, and formation of the four chambers found in the adult. This process is controlled by the spatiotemporal expression of a number of developmental pathways including the heregulin, bone morphogenetic protein, fibroblast growth factor, and Wnt pathways and transcription factors that include targets of these pathways as well as GATA, T-box, and Nkx proteins (33). Targeting of genes in these pathways typically results in abnormal cardiac development.

Similarly, the coordinate expression of multiple developmental pathways is required for normal neural tube closure (reviewed in reference 8), and pathways involved in this and subsequent brain development include sonic hedgehog signaling, Notch, and, again, the Wnt pathway. Neural tube defects are a common developmental abnormality in humans, including spina bifida, when the posterior neural tube fails to close; anencephaly, when the defect is anterior; or craniorachischisis, when the entire neural tube is open. All of these neural tube defects were observed in the CK2α$^{-/-}$ embryos. Closure of the neural tube allows the rapid expansion of brain volume due to fluid pressure exerted on the lumen of the closed neural tube (9, 10, 15, 34, 37, 38); when the neural tube fails to close, the neural tube collapses, as was seen in the CK2α$^{-/-}$ embryos. Neural tube defects, while severe, generally do not lead to embryonic lethality (7).

Thus, one of the pathways that is common to heart and brain development is the Wnt pathway (24–26, 31). The Wnt transcriptional cofactor β-catenin is required for normal heart formation (21), and the Wnt target cripto is required for the differentiation of cardiomyocytes, cardiogenesis, and neural tube formation (11, 29, 49, 50). Targeted deletion of Wnt1 or Wnt3a causes defects in the midbrain and hindbrain regions and ectopic secondary neural tubes, respectively (24–26, 31, 44). Dvl knockouts have defects of closure of the neural folds (48). We have shown that CK2 is a critical regulator of Wnt signaling in cells and in *Xenopus laevis* embryos (12, 42, 43). Thus, the neural tube and heart defects in CK2α$^{-/-}$ embryos could be due, in part, to the dysregulation of the Wnt pathway. Because of the complex developmental regulation of the neural tube and heart, and the many cellular processes regulated by CK2, a precise determination of the mechanisms behind the developmental defects in the CK2α$^{-/-}$ embryos will require a thorough investigation of transcriptional and posttranslational regulation of components of Wnt and other signaling pathways using a variety of genomic and proteomic techniques.

In contrast to the essential role of CK2α in embryogenesis, CK2α′ plays a required role in male germ cell development only (51). Thus, CK2α and CK2α′ are not redundant. This may be due to the fact that CK2α is the more abundant catalytic subunit in the developing embryo, accounting for more than three-fourths of the CK2 catalytic activity. Furthermore, the loss of CK2α leads to diminished CK2β levels in the embryo, similar to what we observed previously with a reduction of CK2α levels in cells using small interfering RNA oligonucleotides (39). Alternatively, the CK2α and CK2α′ subunits may have functional differences; functional specialization of CK2 subunits has been seen in biochemical studies using dominant negative catalytic subunits (47) and through studies identifying unique partners (3). In the future, the issue of functional specialization could be resolved through knock-in experiments by substituting one catalytic subunit for another.

ACKNOWLEDGMENTS

We acknowledge highly skilled technical assistance in carrying out these studies, including Jessica Murray for assistance with ES cell culture, Greg Martin of the Transgenic Core at Boston University Medical Center for carrying out the blastocyst injections, Julie Cha for assistance with analyzing the branchial arch and other embryonic phenotypes, and Patrick Hogan for assistance with mouse colony management. TC1 cells, made by Chuxia Deng and Anthony Wynshaw-Boris, were a kind gift of Philip Leder.

This work was supported by NIH grant R01 CA71796 to D.C.S. as well as project 2 of P01 ES011624 (G. Sonenshein, P.I.), an award from the American Heart Association (0735521T) to I.D., a predoctoral fellowship to D.Y.L. through NIH grant T32 CA064070 (Oncobiology Training Program at Boston University School of Medicine), and a Department of Medicine pilot grant to I.D.

REFERENCES

1. **Ackermann, K., A. Waxmann, C. V. Glover, and W. Pyerin.** 2001. Genes targeted by protein kinase CK2: a genome-wide expression array analysis in yeast. Mol. Cell. Biochem. **227:**59–66.
2. **Bidwai, A. P., J. C. Reed, and C. V. Glover.** 1995. Cloning and disruption of CKB1, the gene encoding the 38-kDa beta subunit of Saccharomyces cerevisiae casein kinase II (CKII). Deletion of CKII regulatory subunits elicits a salt-sensitive phenotype. J. Biol. Chem. **270:**10395–10404.
3. **Bosc, D. G., K. C. Graham, R. B. Saulnier, C. Zhang, D. Prober, R. D. Gietz, and D. W. Litchfield.** 2000. Identification and characterization of CKIP-1, a novel pleckstrin homology domain-containing protein that interacts with protein kinase CK2. J. Biol. Chem. **275:**14295–14306.
4. **Buchou, T., M. Vernet, O. Blond, H. H. Jensen, H. Pointu, B. B. Olsen, C. Cochet, O. G. Issinger, and B. Boldyreff.** 2003. Disruption of the regulatory beta subunit of protein kinase CK2 in mice leads to a cell-autonomous defect and early embryonic lethality. Mol. Cell. Biol. **23:**908–915.
5. **Channavajhala, P., and D. C. Seldin.** 2002. Functional interaction of protein kinase CK2 and c-Myc in lymphomagenesis. Oncogene **21:**5280–5288.
6. **Conway, S. J., A. Kruzynska-Frejtag, P. L. Kneer, M. Machnicki, and S. V. Koushik.** 2003. What cardiovascular defect does my prenatal mouse mutant have, and why? Genesis **35:**1–21.
7. **Copp, A. J.** 1995. Death before birth: clues from gene knockouts and mutations. Trends Genet. **11:**87–93.
8. **Copp, A. J., N. D. Greene, and J. N. Murdoch.** 2003. The genetic basis of mammalian neurulation. Nat. Rev. Genet. **4:**784–793.
9. **Desmond, M. E., and G. C. Schoenwolf.** 1986. Evaluation of the roles of intrinsic and extrinsic factors in occlusion of the spinal neurocoel during rapid brain enlargement in the chick embryo. J. Embryol. Exp. Morphol. **97:**25–46.
10. **Desmond, M. E., and G. C. Schoenwolf.** 1985. Timing and positioning of occlusion of the spinal neurocele in the chick embryo. J. Comp. Neurol. **235:**479–487.
11. **Ding, J., L. Yang, Y. T. Yan, A. Chen, N. Desai, A. Wynshaw-Boris, and M. M. Shen.** 1998. Cripto is required for correct orientation of the anterior-posterior axis in the mouse embryo. Nature **395:**702–707.
12. **Dominguez, I., J. Mizuno, H. Wu, D. H. Song, K. Symes, and D. C. Seldin.** 2004. Protein kinase CK2 is required for dorsal axis formation in Xenopus embryos. Dev. Biol. **274:**110–124.
13. **Ghavidel, A., D. J. Hockman, and M. C. Schultz.** 1999. A review of progress towards elucidating the role of protein kinase CK2 in polymerase III transcription: regulation of the TATA binding protein. Mol. Cell. Biochem. **191:**143–148.
14. **Ghavidel, A., and M. C. Schultz.** 2001. TATA binding protein-associated CK2 transduces DNA damage signals to the RNA polymerase III transcriptional machinery. Cell **106:**575–584.
15. **Gilbert, S. F.** 2003. Developmental biology, 7th ed., p. 838. Sinauer Associates, Sunderland, MA.
16. **Hanna, D. E., A. Rethinaswamy, and C. V. Glover.** 1995. Casein kinase II is required for cell cycle progression during G1 and G2/M in Saccharomyces cerevisiae. J. Biol. Chem. **270:**25905–25914.
17. **Kelliher, M. A., D. C. Seldin, and P. Leder.** 1996. Tal-1 induces T cell acute lymphoblastic leukemia accelerated by casein kinase IIalpha. EMBO J. **15:**5160–5166.
18. **Kubalak, S. W., W. C. Miller-Hance, T. X. O'Brien, E. Dyson, and K. R. Chien.** 1994. Chamber specification of atrial myosin light chain-2 expression precedes septation during murine cardiogenesis. J. Biol. Chem. **269:**16961–16970.
19. **Landesman-Bollag, E., P. L. Channavajhala, R. D. Cardiff, and D. C. Seldin.** 1998. p53 deficiency and misexpression of protein kinase CK2alpha collaborate in the development of thymic lymphomas in mice. Oncogene **16:**2965–2974.
20. **Landesman-Bollag, E., R. Romieu-Mourez, D. H. Song, G. E. Sonenshein, R. D. Cardiff, and D. C. Seldin.** 2001. Protein kinase CK2 in mammary gland tumorigenesis. Oncogene **20:**3247–3257.
21. **Liebner, S., A. Cattelino, R. Gallini, N. Rudini, M. Iurlaro, S. Piccolo, and E. Dejana.** 2004. Beta-catenin is required for endothelial-mesenchymal transformation during heart cushion development in the mouse. J. Cell Biol. **166:**359–367.
22. **Lin, J. M., V. L. Kilman, K. Keegan, B. Paddock, M. Emery-Le, M. Rosbash, and R. Allada.** 2002. A role for casein kinase 2alpha in the Drosophila circadian clock. Nature **420:**816–820.
23. **Mansour, S. L., K. R. Thomas, and M. R. Capecchi.** 1988. Disruption of the proto-oncogene int-2 in mouse embryo-derived stem cells: a general strategy for targeting mutations to non-selectable genes. Nature **336:**348–352.
24. **Mastick, G. S., C. M. Fan, M. Tessier-Lavigne, G. N. Serbedzija, A. P. McMahon, and S. S. Easter, Jr.** 1996. Early deletion of neuromeres in Wnt-1−/− mutant mice: evaluation by morphological and molecular markers. J Comp. Neurol. **374:**246–258.
25. **McMahon, A. P., and A. Bradley.** 1990. The Wnt-1 (int-1) proto-oncogene is required for development of a large region of the mouse brain. Cell **62:**1073–1085.
26. **McMahon, A. P., A. L. Joyner, A. Bradley, and J. A. McMahon.** 1992. The midbrain-hindbrain phenotype of Wnt-1−/Wnt-1− mice results from stepwise deletion of engrailed-expressing cells by 9.5 days postcoitum. Cell **69:**581–595.
27. **Meggio, F., and L. A. Pinna.** 2003. One-thousand-and-one substrates of protein kinase CK2? FASEB J. **17:**349–368.
28. **Miller-Hance, W. C., M. LaCorbiere, S. J. Fuller, S. M. Evans, G. Lyons, C. Schmidt, J. Robbins, and K. R. Chien.** 1993. In vitro chamber specification during embryonic stem cell cardiogenesis. Expression of the ventricular myosin light chain-2 gene is independent of heart tube formation. J. Biol. Chem. **268:**25244–25252.
29. **Morkel, M., J. Huelsken, M. Wakamiya, J. Ding, M. van de Wetering, H. Clevers, M. M. Taketo, R. R. Behringer, M. M. Shen, and W. Birchmeier.** 2003. Beta-catenin regulates Cripto- and Wnt3-dependent gene expression programs in mouse axis and mesoderm formation. Development **130:**6283–6294.
30. **Niefind, K., B. Guerra, I. Ermakowa, and O. G. Issinger.** 2001. Crystal structure of human protein kinase CK2: insights into basic properties of the CK2 holoenzyme. EMBO J. **20:**5320–5331.
31. **Nusse, R., and H. E. Varmus.** 1992 Wnt genes. Cell **69:**1073–1087.
32. **ole-MoiYoi, O. K.** 1989. Theileria parva: an intracellular protozoan parasite that induces reversible lymphocyte transformation. Exp. Parasitol. **69:**204–210.
33. **Olson, E. N.** 2006. Gene regulatory networks in the evolution and development of the heart. Science **313:**1922–1927.
34. **Pacheco, M. A., R. W. Marks, G. C. Schoenwolf, and M. E. Desmond.** 1986. Quantification of the initial phases of rapid brain enlargement in the chick embryo. Am. J. Anat. **175:**403–411.
35. **Rethinaswamy, A., M. J. Birnbaum, and C. V. Glover.** 1998. Temperature-sensitive mutations of the CKA1 gene reveal a role for casein kinase II in maintenance of cell polarity in Saccharomyces cerevisiae. J. Biol. Chem. **273:**5869–5877.
36. **Roussou, I., and G. Draetta.** 1994. The *Schizosaccharomyces pombe* casein kinase II α and β subunits: evolutionary conservation and positive role of the β subunit. Mol. Cell. Biol. **14:**576–586.
37. **Schoenwolf, G. C., and M. E. Desmond.** 1984. Neural tube occlusion precedes rapid brain enlargement. J. Exp. Zool. **230:**405–407.
38. **Schoenwolf, G. C., and M. E. Desmond.** 1986. Timing and positioning of reopening of the occluded spinal neurocele in the chick embryo. J. Comp. Neurol. **246:**459–466.
39. **Seldin, D. C., E. Landesman-Bollag, M. Farago, N. Currier, D. Lou, and I. Dominguez.** 2005. CK2 as a positive regulator of Wnt signalling and tumourigenesis. Mol. Cell. Biochem. **274:**63–67.
40. **Seldin, D. C., and P. Leder.** 1995. Casein kinase II alpha transgene-induced murine lymphoma: relation to theileriosis in cattle. Science **267:**894–897.
41. **Snell, V., and P. Nurse.** 1994. Genetic analysis of cell morphogenesis in fission yeast—a role for casein kinase II in the establishment of polarized growth. EMBO J. **13:**2066–2074.
42. **Song, D. H., I. Dominguez, J. Mizuno, M. Kaut, S. C. Mohr, and D. C. Seldin.** 2003. CK2 phosphorylation of the armadillo repeat region of beta-catenin potentiates Wnt signaling. J. Biol. Chem. **278:**24018–24025.
43. **Song, D. H., D. J. Sussman, and D. C. Seldin.** 2000. Endogenous protein kinase CK2 participates in Wnt signaling in mammary epithelial cells. J. Biol. Chem. **275:**23790–23797.
44. **Takada, S., K. L. Stark, M. J. Shea, G. Vassileva, J. A. McMahon, and A. P. McMahon.** 1994. Wnt-3a regulates somite and tailbud formation in the mouse embryo. Genes Dev. **8:**174–189.
45. **Toselli, P., B. Faris, D. Sassoon, B. A. Jackson, and C. Franzblau.** 1992. In-situ hybridization of tropoelastin mRNA during the development of the multilayered neonatal rat aortic smooth muscle cell culture. Matrix **12:**321–332.
46. **Unger, G. M., A. T. Davis, J. W. Slaton, and K. Ahmed.** 2004. Protein kinase

CK2 as regulator of cell survival: implications for cancer therapy. Curr. Cancer Drug Targets **4:**77–84.

47. **Vilk, G., R. B. Saulnier, R. St. Pierre, and D. W. Litchfield.** 1999. Inducible expression of protein kinase CK2 in mammalian cells. Evidence for functional specialization of CK2 isoforms. J. Biol. Chem. **274:**14406–14414.
48. **Wang, J., N. S. Hamblet, S. Mark, M. E. Dickinson, B. C. Brinkman, N. Segil, S. E. Fraser, P. Chen, J. B. Wallingford, and A. Wynshaw-Boris.** 2006. Dishevelled genes mediate a conserved mammalian PCP pathway to regulate convergent extension during neurulation. Development **133:**1767–1778.
49. **Xu, C., G. Liguori, E. D. Adamson, and M. G. Persico.** 1998. Specific arrest of cardiogenesis in cultured embryonic stem cells lacking Cripto-1. Dev. Biol. **196:**237–247.
50. **Xu, C., G. Liguori, M. G. Persico, and E. D. Adamson.** 1999. Abrogation of the Cripto gene in mouse leads to failure of postgastrulation morphogenesis and lack of differentiation of cardiomyocytes. Development **126:**483–494.
51. **Xu, X., P. A. Toselli, L. D. Russell, and D. C. Seldin.** 1999. Globozoospermia in mice lacking the casein kinase II alpha′ catalytic subunit. Nat. Genet. **23:**118–121.